analytical chemistry

pubs.acs.org/ac Article

Stochastic DNA Dual-Walkers for Ultrafast Colorimetric Bacteria Detection

Haihong Yang, Mingshu Xiao, Wei Lai, Ying Wan, Li Li, and Hao Pei*

Cite This: *Anal. Chem.* 2020, 92, 4990−4995 Read Online

ACCESS | Metrics & More | Article Recommendations | Supporting Information

ABSTRACT: Rapid, sensitive, and reliable pathogen detection is growing in importance in human health and safety. In this work, we report a stochastic DNA dual-walker-based colorimetric biosensor for bacterial detection. In the presence of target bacteria, two kinds of released multiple walking strands are allowed for continuous walking on the Au nanoparticle (AuNP)-based 3D track, resulting in destabilized aggregation of AuNP-based probes. The induced color change from red to blue can serve as an analytical signal for colorimetric detection of target bacteria. We demonstrated that this mothed enables sensitive and specific bacterial detection within 15 min due to its ultrafast reaction kinetics and sensitive color change, showing a linear response ranging from 10^0 to 10^5 CFU/mL with a limit of detection of 1 CFU/mL. Moreover, we also realized analysis of practical samples using this colorimetric biosensor. Given its features of rapid, sensitive, specific, and reliable analysis, our stochastic dual-walker-based colorimetric biosensor shows much promise in point-of-care testing for bacteria detection.

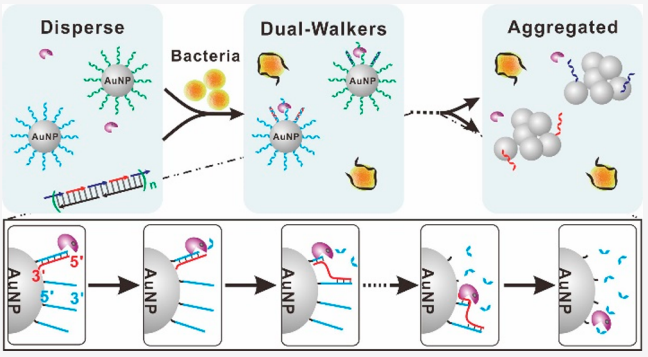

Downloaded via CARLETON UNIV on July 16, 2020 at 20:23:48 (UTC).
See https://pubs.acs.org/sharingguidelines for options on how to legitimately share published articles.

Bacterial infections have been emerging as a huge burden on public health,[1,2] causing approximately one-fifth of all deaths worldwide each year.[3] For this issue, accurate and early detection of bacterial pathogens is key to the control of infectious diseases.[4,5] Despite the fact that the most commonly used tools, such as colony counting,[6] the enzyme-linked immunosorbent assay,[7,8] and polymerase chain reaction,[9] are available for sensitive detection of pathogens, most of these methods require long processing times (over 18 h from sampling to results) and specialized equipment, which are not conducive to rapid detection of bacteria.[10] Accordingly, this slow time to answer provides a powerful impetus to develop rapid, sensitive, and reliable methods for bacterial detection in the early stage of bacterial infection,[11−13] thus improving the patient survival rates.

Functionalized gold nanoparticle (AuNP)-based colorimetric biosensing has elicited a growing interest in diagnostics, antibioterrorism, and environmental monitoring because of their easy readout, portability, and cost-efficiency.[14−18] In general, their color change from red to blue arises from interparticle surface plasmon coupling induced by the reduced distance between AuNPs. By exploitation of this corresponding color change as an analytical signal, AuNP-based colorimetric biosensors have been developed for detection of various targets (e.g., DNA, heavy metal ions, proteins, bacteria, viruses, cancer cells).[19−23] Nevertheless, the sluggish response and the poor detection limits remain as bottleneck constraints for their practical applications (e.g., point-of-care testing).[24,25] The sluggish response related to slow reaction kinetics often leads to time-consuming analytical processes whereas a lack of signal amplification strategies is responsible for the limited detection limits. For example, an AuNP-based microfluidic biosensor developed by Zheng et al. enables colorimetric detection of 50 CFU/mL *Escherichia coli* O157:H7 within 1 h,[26] but its detection time and detection limit can be further improved by higher reaction efficiency and signal amplification for meeting the demand of practical use in food safety. Hence, AuNP-based colorimetric biosensors with sensitive color changes allowing for rapid and sensitive detection of bacteria are of great significance.

Recently, our group constructed an analytical platform based on enzyme-driven stochastic DNA walkers for bacteria detection.[27] The autonomous and progressive walk on a AuNP-based three dimentional (3D) track enables the transduction and amplification of biorecognition signals.[28−30] As a result, such an enzyme-assisted cascade signal amplification strategy makes this walker-based sensor platform achieve single-bacteria analysis ability. Nevertheless, this

Received: November 12, 2019
Accepted: March 13, 2020
Published: March 13, 2020

© 2020 American Chemical Society

https://dx.doi.org/10.1021/acs.analchem.9b05149
Anal. Chem. 2020, 92, 4990−4995

analytical platform requires relatively long processing time (about 4 h) to acquire a saturated fluorescent signal. Therefore, to achieve ultrafast and sensitive bacteria analysis, we developed a stochastic DNA dual-walker-based colorimetric biosensor. As illustrated in Figure 1, two kinds of probes

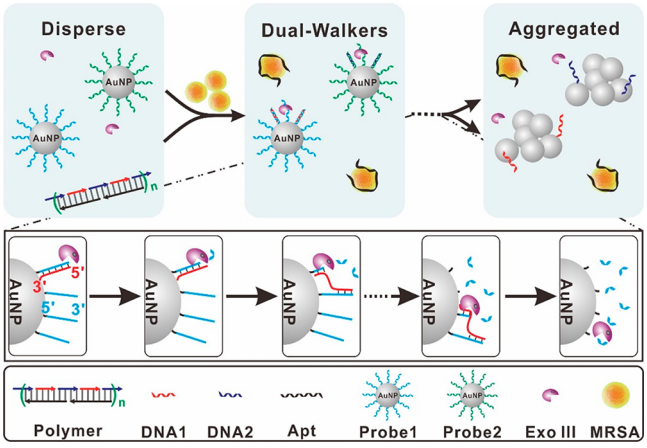

Figure 1. Schematic illustration of stochastic DNA dual-walkers for colorimetric detection of bacteria.

composed of thiol-tagged oligonucleotide-functionalized AuNPs were designed and well-dispersed in the system. Due to their high affinity, the aptamer (black strands) can bind to bacteria in the presence of target bacteria, concomitantly releasing two kinds of walking strands (red and blue strands). Propelled by Exo III through consumption of thiol-tagged oligonucleotides, the released walking strands are allowed for autonomous walk on the AuNP-based 3D track. Moreover, multiple-step walking behavior arising from multiple cycles of hybridization and digestion results in destabilized aggregation of probes, and their induced color change from red to blue can serve as an analytical signal for quantitative analysis of bacteria. More importantly, the operation of DNA dual-walkers in one system is capable of accelerating the enzyme digestion reaction, thus shortening response time and speeding the analytical procedure. In addition, multiple walking strands concurrently released from one polymer would further improve reaction kinetics. Therefore, our stochastic dual-walker-based sensor with ultrafast reaction kinetic shows sensitive color changes and is anticipated to provide a simple-yet-effective tool for ultrafast and sensitive colorimetric bacteria detection.

EXPERIMENTAL SECTION

Reagents and Materials. $HAuCl_4{\cdot}4H_2O$ used for AuNP synthesis was purchased from Shanghai Chemical Reagent Company (Shanghai, China). Phosphate-buffered saline and trisodium citrate were supplied by Sigma-Aldrich, Israel. Exo III was obtained from TaKaRa Biotechnology Co., Ltd. (Dalian, China). The MRSA aptamer and DNA were synthesized by Sangon Biotech Co. Ltd. (Shanghai, China) with standard desalting, purified with HPLC, and used without further purification. All the solutions were prepared using ultrapure water with a resistivity of 18.2 $M\Omega{\cdot}cm^{-1}$ purified by a Milli-Q system (Hitachi, Japan).

Methicillin-resistant *Staphylococcus aureus* (MRSA, ATCC BAA 1766) was provided by China General Microbiological Culture Collection Center. *Pseudomonas aeruginosa* (*P. aeru*, CMCC 10102), Shigella (CMCC 51572), and *Escherichia coli* (*E. coli*, CMCC 44103) were purchased from China Center for Type Culture Collection.

Preparation of Probes. Citrate-stabilized AuNPs (a size of 13 nm) were synthesized based on previous procedures.[31,32] Briefly, 3.5 mL of trisodium citrate (1 wt %) was rapidly injected into a boiling solution of 100 mL of $HAuCl_4$ (0.01 wt %) under stirring. Then the solution was refluxed for another 10 min after the color changed from pale yellow to deep red. The obtained citrate-stabilized AuNPs were stored at 4 °C for further assay.

To construct probes, the prepared AuNPs were first functionalized with thiolated probe strand 1 (or probe strand 2, probe strand 3, probe strand 4) using a pH-assisted and surfactant-free route.[33,34] In brief, 4 μL of thiolated oligonucleotides (100 μM) were added into 100 μL of AuNPs (10 nM), followed by dropping 2 μL of citrate-HCl (500 mM, pH = 3) buffer into the mixture. After incubation for 20 min, the solution was centrifuged (12000 rpm, 15 min, 15 °C) to remove the unmodified DNA; the precipitate was washed three times with PBS and finally dispersed in 100 μL of PBS (10 mM, pH = 7.4). The concentration of the probes was determined by measuring their absorbance at 521 nm.

Preparation of Polymer. The aptamer, DNA1, and DNA2 were dissolved in TAE buffer (10 mM Tris-HCl and 50 mM $MgCl_2$, pH = 7.0), yielding a final concentration of 100 μM. One microliter of each strand was combined with 97 μL of TAE buffer, and the resulting mixture was heated to 95 °C for 5 min and then cooled to 25 °C in 2 h with a Peltier thermal cycler PTC-200 (MJ Research Inc., SA).

PAGE Gel Electrophoresis. The 8% PAGE gels were prepared with 1× TBE buffer (40 mM Tris-borate and 1 mM EDTA, pH 7.0) and were run at 120 V for 60 min and visualized under UV light.

Bacteria Culture and Counting. The exact number of bacteria was counted by plating 10 μL of appropriate dilution onto the Mueller−Hinton agar according to plate-counting method. Bacteria were cultured in Luria−Bertani broth medium at 37 °C for overnight under continuous shaking and then centrifuged (3500 rpm, 5 min, 4 °C), and the bacteria were washed with PBS three times. After incubation at 37 °C for 24 h, the number of colony forming units per milliliter (CFU/mL) was determined by counting the colonies grown on the plates.

Procedure for Colorimetric Assays. A typical colorimetric assay was carried out as follows. MRSA with a final concentration of 10^5 CFU/mL was added into phosphate buffer (1 mL, 10 mM, pH = 7.0) containing 1 μM polymer, Exo III (0.5 U/μL), and 4 nM probes (2 nM of each kind of probes). After Exo III-triggered DNA walking at 37 °C, the UV−vis absorption spectra with a wavelength range of 300 to 800 nm were recorded using an Agilent Cary60 spectrophotometer (Agilent Technologies, Santa Clara, CA).

Kinetic Study. Once MRSA with a final concentration of 10^6 CFU/mL was added into PBS solution (1 mL, containing 4 nM probes, 1 μM polymer, and 0.5 U/μL Exo III), its absorption spectrum was rapidly recorded using a UV−visible spectrometer, followed by monitoring for every 1 min.

Colorimetric Detection of MRSA. The sample solution containing different concentrations of MRSA (a final concentration of 1 to 10^8 CFU/mL) was added to phosphate buffer (1 mL, 10 mM, pH = 7.0) containing 10 nM polymer, 0.5 U/μL Exo III, and 4 nM probes (2 nM of each kind of probes). After incubation at 37 °C for 15 min, the absorption

https://dx.doi.org/10.1021/acs.analchem.9b05149
Anal. Chem. 2020, 92, 4990−4995

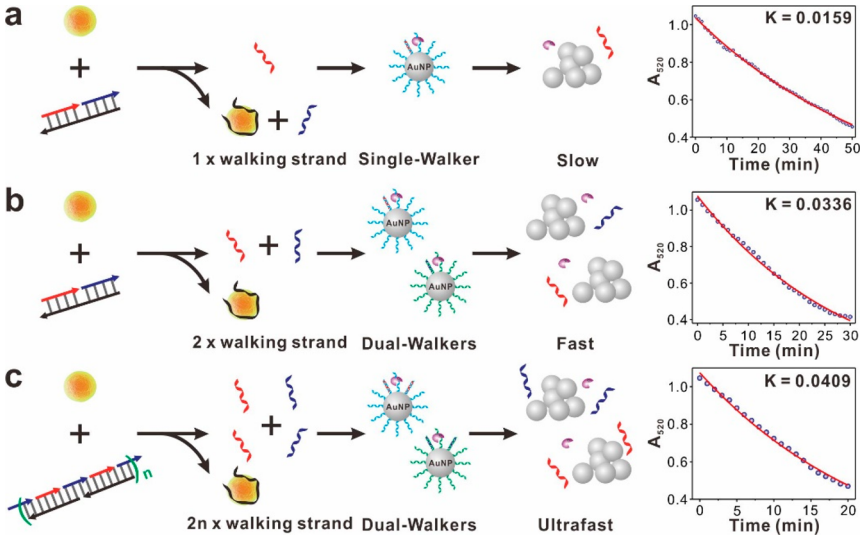

Figure 2. Scheme of three modes for colorimetric bacterial analysis (left) and their kinetic curves (right). (a) Mode 1: single-walker with 1× walking strands, (b) mode 2: dual-walkers with 2× walking strands, and (c) mode 3: dual-walkers with 2*n*× walking strands.

spectra were measured. To demonstrate specificity, a control experiment was carried out in the same manner as mentioned above, except that MRSA (10^6 CFU/mL) was replaced by 10^8 CFU/mL nonspecific bacteria (i.e, *P. aeru*, *Shigella*, *E. coli*).

RESULTS AND DISCUSSION

Given that AuNP-based colorimetric biosensing with fast response time is conducive to rapid detection of bacteria, we proposed AuNP-based colorimetric biosensors in three modes (i.e., single-walker with 1× walking strands (mode 1), dual-walkers with 2× walking strands (mode 2), and dual-walkers with 2*n*× walking strands (mode 3)) for bacterial analysis (Figure 2). As illustrated in Figure 2a (left), only the released DNA1 (labeled with red) serves as walking strand when in the presence of target bacteria and moves along the AuNP-based 3D track powered by Exo III. Thereafter, multiple-step walking behavior results in destabilized aggregation of probes and thus leads to color change. As a result of single-walker with 1× walking strands, the enzyme digestion kinetics of mode 1 is relative slow, reflecting that a long time (50 min) is required for observation of the visualized blue color (Figure S3). While conducting bioassays in mode 2 (Figure 2b, left), both the released DNA1 and DNA2 (labeled with red and blue, respectively) are utilized as walking strands and allowed for walking their corresponding 3D track (two kinds of probes used here). The kinetic study demonstrated that the simultaneous operation of dual-walkers accelerates the enzyme digestion reaction, exhibiting the observed blue color in 30 min (Figure S3).

To further speed the kinetics, the assay was implemented in mode 3. Prior to implementation, hybridization chain reaction (HCR) product termed polymer was synthesized on the basis of HCR (Figure S1), whose formation was verified by gel electrophoresis analysis (Figure S2). When exploiting mode 3 for colorimetric detection, the presence of target bacteria would induce release of 2*n*× walking strands from one polymer (Figure 2c, left). As such, in addition to operation of dual-walkers just like in mode 2, the increasing amount of released walking strands would further accelerate enzyme digestion reaction. As a result, the color of probes changing from red to blue can be observed in only 20 min (Figure S3), greatly reducing the response time (from 50 to 20 min). The assays conducted in mode 3 with ultrafast response time are in favor of AuNP-based colorimetric detection of bacteria.

To gain deep insight, we fitted the kinetic curves of the three modes with the first-order kinetic equation:[35,36]

$$A = A_0 \exp(-kt)$$

where t is the enzyme digestion time, and k is reaction rate constant reflecting the rate of enzyme digestion. As shown in Figure 2 (right), the parameter (k) was estimated to be 0.0159 (mode 1), 0.0336 (mode 2), and 0.0409 (mode 3), respectively. Notably, the larger k value indicates faster kinetics, which is related to the number of kinds of DNA walkers and the amount of released walking strands. In view of its ultrafast reaction kinetics, the AuNP-based colorimetric biosensor in mode 3 was thus selected for subsequent bacteria analysis.

The ultrafast kinetics of the DNA machine offers a simple-yet-effective approach to rapid colorimetric bioassays. To test its feasibility, dual-walkers with 2*n*× walking strands were first utilized for colorimetric detection of methicillin-resistant *Staphylococcus aureus* (MRSA). Initially, the UV−vis spectrum of probes displayed a strong absorption peak at 520 nm (Figure 3a). Their absorbance peaks showed no or negligible change after addition of polymer or polymer + MRSA (10^5

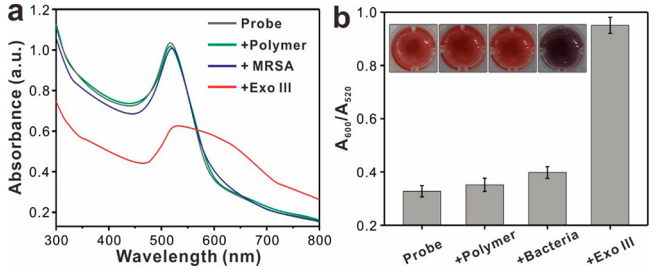

Figure 3. (a) The absorption spectra of probes, probes + polymer, probes + polymer + MRSA, and probes + polymer + MRSA + Exo III. (b) The absorbance ratio of 600 nm over 520 nm (A_{600}/A_{520}) for probes, probes + polymer, probes + polymer + MRSA, and probes + polymer + MRSA + Exo III. Inset: their corresponding photographs.

https://dx.doi.org/10.1021/acs.analchem.9b05149
Anal. Chem. 2020, 92, 4990−4995

CFU/mL) whereas the greatly reduced absorption peak at 520 nm was discovered in the presence of polymer + MRSA + Exo III, concomitant with the appearance of the new peak at ~600 nm. In this case, the color of AuNP-based probes changed from red to blue after 15 min incubation (Figure 3b, inset), which is attributed to Exo III-propelled DNA walking on the AuNP-based 3D track in mode 3 for rapidly inducing the destabilized aggregation of probes. Compared with the well-dispersed AuNPs (Figure S4), AuNP-based probes were aggregated after DNA walker-induced deprotection (Figure S5). On the contrary, other groups presented no color change of probes. Moreover, Exo III-mediated signal amplification resulted in the great enhancement in the absorbance ratio of 600 nm over 520 nm (A_{600}/A_{520}) (Figure 3b). Accordingly, all of these results suggest the feasibility of dual-walkers in mode 3 for colorimetric bacteria detection.

Prior to exploitation of this DNA dual-walker-based colorimetric biosensor for quantitative analysis of bacteria, Exo III concentration was optimized to achieve the best analytical performance. We found the optimized digestion efficiency with Exo III concentration of 0.5 U/μL (Figure S6). Under optimized experimental conditions, we next studied the detection performance of DNA dual-walker-based colorimetric biosensor. As shown in Figure 4a, a colorimetric biosensor in

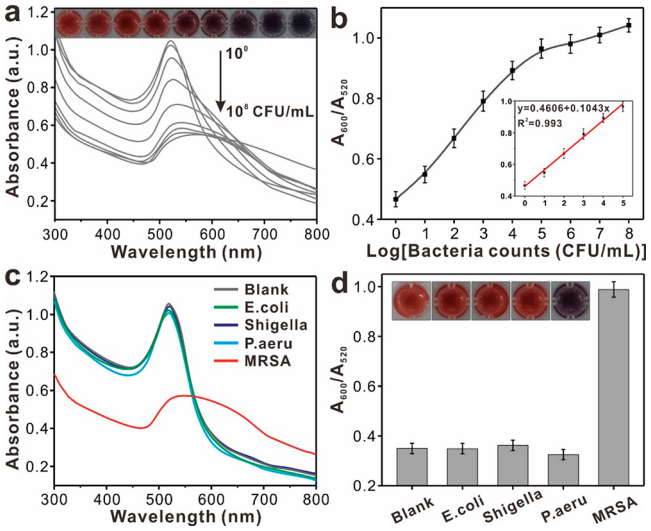

Figure 4. (a) The absorbance spectra of AuNP-based probes in response to different concentration of target MRSA (1 to 10^8 CFU/mL). Inset: their corresponding photographs. (b) The curve for the relationship between A_{600}/A_{520} and the concentration of MRSA. Inset: linear relationship between A_{600}/A_{520} and the concentration of MRSA. (c) The absorbance spectra and (d) A_{600}/A_{520} of AuNP-based probes with different targets. Inset: their corresponding photographs.

reponse to a series of different concentrations of MRSA (10^0 to 10^8 CFU/mL) was recorded using UV−vis spectra. It is found that absorption intensity at 520 nm exhibited a gradual decrease with an increasing concentration of target bacteria, which is consistent with their color change (Figure 4a, inset), revealing the gradual aggregation of probes. Additionally, we investigated the correlation of A_{600}/A_{520} with bacterial concentration and discovered a good linear range from 10^0 to 10^5 CFU/mL (R^2 = 0.993) with a limit of detection (LOD) of 1 CFU/mL (Figure 4b), which is much lower than that of previous colorimetric biosensors for bacteria (see Table 1).[13,37−39] Our proposed method with such high sensitivity is ascribed to a single bacterium that enables release of multiple walking strands and thus induces continuous multiple-step walking behavior of walkers on AuNP-based probes. Moreover, it is worth mentioning that this constructed biosensor with ultrafast reaction kinetics greatly reduces detection time, allowing observation of color change of the AuNP-based probes in ~15 min, which is far lower than the detection time of other colorimetric biosensors.[40−44] Notably, kinetics for high concentrations (>10^5 CFU/mL) different from the lower concentrations might be attributed to more bacteria inducing more released walking strands that are easier to induce rapid aggregation of probes.

To assess the specificity of our colorimetric biosensor for MRSA detection, we carried out control experiments using three kinds of nontarget bacteria including *E. coli*, *Shigella*, and *P. aeru*. UV−vis spectra in Figure 4c indicated that their absorbance peaks showed no obvious change even in high concentration of 10^8 CFU/mL by comparison with the background (blank group). A change in color was also not observed in their corresponding photographs (Figure 4d, inset). In addition, A_{600}/A_{520} of control groups is much lower than that of target MRSA with a concentration of 10^6 CFU/mL (Figure 4d), suggesting that our constructed colorimetric biosensor has superior selectivity. The good selectivity of our method stems from the high recognition capability of aptamer in the polymer to its target. Taking these results together, it is concluded that this dual-walker-based colorimetric biosensor enables specific detection of bacteria.

Next, this colorimetric biosensor was applied in real sample analysis. Hence, we constructed four kinds of simulated samples including cerebrospinal fluid (CSF) sample, urine sample, split sample, and serum sample. Typically, the diluted sample was spiked with concentration of 10^6 CFU/mL bacteria, and their UV−vis spectra were measured with the proposed method. It is found that the absorbance peak at 520 nm was greatly decreased and the color of solution changed into blue only in the presence of target bacteria (i.e., MRSA) (Figure S7 and Figure 5, left), corresponding to significant enhancement of the value of A_{600}/A_{520} (Figure 5, right). Moreover, a recovery assay was conducted to further verify the feasibility of the method for practical applications. As shown in Table S2, the recoveries of standard addition were achieved ranging from 97.5 to 110%, suggesting satisfactory accuracy of the colorimetric biosensor. Nonetheless, a high concentration of nontarget bacteria can also produce a weak signal in practical samples, which might arise from nonspecific adsorption on probes. In the case that the target is in low concentration (<10^3 CFU/mL), a high concentration of nontarget bacteria would interfere with detection, which yet would not hamper the determination of high concentration target bacteria (≥10^3 CFU/mL). To address this issue, the competing adsorption could potentially be suppressed by modifying the probes with bovine serum albumin or 6-mercapto-1-hexanol as sealing agent.[49−51] To sum up, all of these results disclose that this dual-walker-based colorimetric method holds great potential for practical applications in complex biological samples under a given condition.

Our previous reported stochastic DNA walker-based analytical platform enables single bacterium analysis because of enzyme-assisted cascade signal amplification, but this method is restricted by its relative long processing time and analyzed with specialized equipment. Here, to accelerate reaction kinetic and shorten response time, stochastic DNA

https://dx.doi.org/10.1021/acs.analchem.9b05149
Anal. Chem. 2020, 92, 4990−4995

Table 1. Comparison of Different Methods for Colorimetric Detection of Bacteria

detection method	analyte	linear range	LOD	analysis time	ref
colorimetric	*Staphylococcus aureus*	1 to 10^5 CFU/mL	1 CFU/mL	~15 min	this work
colorimetric	*Escherichia coli*	—	100 CFU/mL	<60 min	13
colorimetric	*Escherichia coli*	10^3 to 10^6 CFU/mL	41 CFU/mL	~95 min	37
colorimetric	*Escherichia coli*	—	10^4 CFU/mL	10 min	6
colorimetric	*Staphylococcus aureus*	1.5×10^2 to 1.5×10^6 CFU/mL	1.5×10^3 CFU/mL in PBS	40 min	39
		—	1.5×10^5 CFU in the milk sample		
colorimetric	*Escherichia coli*	—	1×10^5 CFU/mL	2 h	42
colorimetric	*Staphylococcus aureus*	50 to 10^4 CFU/mL	20 CFU/mL	>80 min	43
colorimetric	*Listeria monocytogenes*	—	2.17×10^2 CFU/mL	18 h	45
colorimetric	*Escherichia coli*	—	10 CFU/mL	26 min	44
colorimetric	*E. coli*	—	30 CFU/mL	<60 min	46
	S. aureus	—	200 CFU/mL		
colorimetric	*Salmonella enteritidis*	—	10^3 CFU/mL	2 h	47
colorimetric	*Salmonella typhimuriumusing*	0 to 2×10^4 cells	2×10^1 cells/g	45 min	48

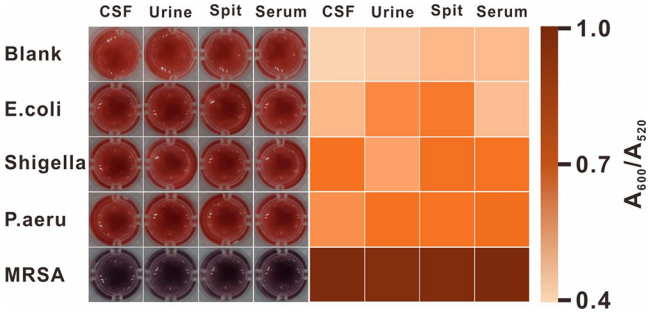

Figure 5. Photographs (right) and A_{600}/A_{520} (left) of AuNP-based probes with different targets in CSF samples, urine samples, spit samples, and serum samples.

dual-walkers were introduced into one system. By integrating ultrafast reaction kinetic of dual-walkers with AuNP-based colorimetric biosensing, we achieved rapid, sensitive, and reliable detection of bacteria. As a result, our constructed method with easy readout, portability, and cost efficiency shows much promise as a point-care-of-testing tool for accurate and early detection of bacterial pathogens.

CONCLUSION

In summary, we have exploited stochastic DNA dual-walkers for construction of a colorimetric biosensor for bacteria detection. This dual-walker-based colorimetric biosensor presents several distinctive advantages over other colorimetric biosensors for bacteria. First, this work offers a facile and efficient approach to construct AuNP-based colorimetric bacteria biosensor. Second, as a result of dual walkers in combination with multiple walking strands for continuous walk on a AuNP-based 3D track propelled by enzyme, our biosensor with ultrafast reaction kinetics shows sensitive color change in response to target bacteria, achieving rapid quantitative analysis in ~15 min. Third, this method enables sensitive and specific bacterial detection, presenting a linear range from 10^0 to 10^5 CFU/mL with LOD of 1 CFU/mL. Moreover, we also demonstrated that the colorimetric assay can be applied for analysis of practical samples. Collectively, our stochastic dual walker-based colorimetric biosensor, enabling ultrafast and sensitive colorimetric bacteria detection, holds great potential as point-of-care testing tools for on-site bacterial analysis.

ASSOCIATED CONTENT

Supporting Information

The Supporting Information is available free of charge at https://pubs.acs.org/doi/10.1021/acs.analchem.9b05149.

Scheme of employing HCR to synthesize polymer (Figure S1), PAGE gel electrophoresis showing the self-assembly of polymer (Figure S2), the absorbance spectra of Mode 1, Mode 2, and Mode 3 (Figure S3), TEM image of AuNPs (Figure S4), TEM image of aggregated AuNP-based probes (Figure S5), the optimized assays for Exo III concentration (Figure S6), the absorbance spectra of AuNP aggregates with different targets in practical samples (Figure S7), the nucleic acids used in this work (Table S1), recovery results of MRSA in human serum (Table S2) (PDF)

AUTHOR INFORMATION

Corresponding Author

Hao Pei − *Shanghai Key Laboratory of Green Chemistry and Chemical Processes, School of Chemistry and Molecular Engineering, East China Normal University, Shanghai 200241, China;* orcid.org/0000-0002-6885-6708; Email: peihao@chem.ecnu.edu.cn

Authors

Haihong Yang − *Shanghai Key Laboratory of Green Chemistry and Chemical Processes, School of Chemistry and Molecular Engineering, East China Normal University, Shanghai 200241, China*

Mingshu Xiao − *Shanghai Key Laboratory of Green Chemistry and Chemical Processes, School of Chemistry and Molecular Engineering, East China Normal University, Shanghai 200241, China;* orcid.org/0000-0003-0673-1544

Wei Lai − *Shanghai Key Laboratory of Green Chemistry and Chemical Processes, School of Chemistry and Molecular Engineering, East China Normal University, Shanghai 200241, China*

Ying Wan − *School of Mechanical Engineering, Nanjing University of Science and Technology, Nanjing 210094, China*

Li Li − *Shanghai Key Laboratory of Green Chemistry and Chemical Processes, School of Chemistry and Molecular Engineering, East China Normal University, Shanghai 200241, China;* orcid.org/0000-0001-8494-4997

Complete contact information is available at:

https://dx.doi.org/10.1021/acs.analchem.9b05149
Anal. Chem. 2020, 92, 4990−4995

https://pubs.acs.org/10.1021/acs.analchem.9b05149

Notes

The authors declare no competing financial interest.

■ ACKNOWLEDGMENTS

This work was supported by the National Science Foundation of China (grant no. 21722502), National Key Research and Development Program of China for International Science & Innovation Cooperation Major Project between Governments (2018YFE0113200), Shanghai Rising-Star Program (19QA1403000), and Shanghai Science and Technology Committee (STCSM) (grant no. 18490740500).

■ REFERENCES

(1) Rohr, J. R.; Barrett, C. B.; Civitello, D. J.; Craft, M. E.; Delius, B.; DeLeo, G. A.; Hudson, P. J.; Jouanard, N.; Nguyen, K. H.; Ostfeld, R. S.; Remais, J. V.; Riveau, G.; Sokolow, S. H.; Tilman, D. *Nat. Sustain.* **2019**, *2*, 445−456.
(2) Jones, K. E.; Patel, N. G.; Levy, M. A.; Storeygard, A.; Balk, D.; Gittleman, J. L.; Daszak, P. *Nature* **2008**, *451*, 990−993.
(3) Furuse, Y. *Proc. Natl. Acad. Sci. U. S. A.* **2019**, *116*, 478−483.
(4) Wood, C. S.; Thomas, M. R.; Budd, J.; Mashamba-Thompson, T. P.; Herbst, K.; Pillay, D.; Peeling, R. W.; Johnson, A. M.; McKendry, R. A.; Stevens, M. M. *Nature* **2019**, *566*, 467−474.
(5) Ray, P. C.; Khan, S. A.; Singh, A. K.; Senapati, D.; Fan, Z. *Chem. Soc. Rev.* **2012**, *41*, 3193−3209.
(6) Miranda, O. R.; Li, X.; Garcia-Gonzalez, L.; Zhu, Z.-J.; Yan, B.; Bunz, U. H.; Rotello, V. M. *J. Am. Chem. Soc.* **2011**, *133*, 9650−9653.
(7) Ravan, H.; Yazdanparast, R. *Anal. Chim. Acta* **2012**, *733*, 64−70.
(8) Chen, R.; Huang, X.; Xu, H.; Xiong, Y.; Li, Y. *ACS Appl. Mater. Interfaces* **2015**, *7*, 28632−28639.
(9) Belgrader, P.; Benett, W.; Hadley, D.; Richards, J.; Stratton, P.; Mariella, R.; Milanovich, F. *Science* **1999**, *284*, 449−450.
(10) Slomovic, S.; Pardee, K.; Collins, J. J. *Proc. Natl. Acad. Sci. U. S. A.* **2015**, *112*, 14429−14435.
(11) Varadi, L.; Luo, J. L.; Hibbs, D. E.; Perry, J. D.; Anderson, R. J.; Orenga, S.; Groundwater, P. W. *Chem. Soc. Rev.* **2017**, *46*, 4818−4832.
(12) Ahmed, A.; Rushworth, J. V.; Hirst, N. A.; Millner, P. A. *Clin. Microbiol. Rev.* **2014**, *27*, 631−646.
(13) Peng, H.; Chen, I. A. *ACS Nano* **2019**, *13*, 1244−1252.
(14) Yoo, S. M.; Lee, S. Y. *Trends Biotechnol.* **2016**, *34*, 7−25.
(15) Wu, Z.; Wu, Z.-K.; Tang, H.; Tang, L.-J.; Jiang, J.-H. *Anal. Chem.* **2013**, *85*, 4376−4383.
(16) Baetsen-Young, A. M.; Vasher, M.; Matta, L. L.; Colgan, P.; Alocilja, E. C.; Day, B. *Biosens. Bioelectron.* **2018**, *101*, 29−36.
(17) Chang, C.-C.; Chen, C.-Y.; Chuang, T.-L.; Wu, T.-H.; Wei, S.-C.; Liao, H.; Lin, C.-W. *Biosens. Bioelectron.* **2016**, *78*, 200−205.
(18) Man, T.; Ji, W.; Liu, X.; Zhang, C.; Li, L.; Pei, H.; Fan, C. *ACS Nano* **2019**, *13*, 4826−4833.
(19) Saha, K.; Agasti, S. S.; Kim, C.; Li, X.; Rotello, V. M. *Chem. Rev.* **2012**, *112*, 2739−2779.
(20) Song, Y.; Wei, W.; Qu, X. *Adv. Mater.* **2011**, *23*, 4215−4236.
(21) Xue, X.; Wang, F.; Liu, X. *J. Am. Chem. Soc.* **2008**, *130*, 3244−3245.
(22) Peng, Y.; Li, L.; Mu, X.; Guo, L. *Sens. Actuators, B* **2013**, *177*, 818−825.
(23) Pei, H.; Sha, R.; Wang, X.; Zheng, M.; Fan, C.; Canary, J. W.; Seeman, N. C. *J. Am. Chem. Soc.* **2019**, *141*, 11923−11928.
(24) Priyadarshini, E.; Pradhan, N. *Sens. Actuators, B* **2017**, *238*, 888−902.
(25) Verma, M. S.; Rogowski, J. L.; Jones, L.; Gu, F. X. *Biotechnol. Adv.* **2015**, *33*, 666−680.
(26) Zheng, L.; Cai, G.; Wang, S.; Liao, M.; Li, Y.; Lin, J. *Biosens. Bioelectron.* **2019**, *124*, 143−149.
(27) Xiao, M.; Zou, K.; Li, L.; Wang, L.; Tian, Y.; Fan, C.; Pei, H. *Angew. Chem.* **2019**, *131*, 15594−15600.
(28) Qu, X.; Zhu, D.; Yao, G.; Su, S.; Chao, J.; Liu, H.; Zuo, X.; Wang, L.; Shi, J.; Wang, L.; Huang, W.; Pei, H.; Fan, C. *Angew. Chem., Int. Ed.* **2017**, *56*, 1855−1858.
(29) Xiao, M.; Wang, X.; Li, L.; Pei, H. *Anal. Chem.* **2019**, *91*, 11253−11258.
(30) Xiao, M.; Lai, W.; Man, T.; Chang, B.; Li, L.; Chandrasekaran, A. R.; Pei, H. *Chem. Rev.* **2019**, *119*, 11631−11717.
(31) Hill, H. D.; Mirkin, C. A. *Nat. Protoc.* **2006**, *1*, 324−336.
(32) Shen, J. L.; Liang, L.; Xiao, M. S.; Xie, X. D.; Wang, F.; Li, Q.; Ge, Z. L.; Li, J.; Shi, J. Y.; Wang, L. H.; Li, L.; Pei, H.; Fan, C. H. *J. Am. Chem. Soc.* **2019**, *141*, 11938−11946.
(33) Zhang, X.; Servos, M. R.; Liu, J. *J. Am. Chem. Soc.* **2012**, *134*, 7266−7269.
(34) Xiao, M.; Lai, W.; Wang, F.; Li, L.; Fan, C.; Pei, H. *J. Am. Chem. Soc.* **2019**, *141*, 20354−20364.
(35) Gao, W. Y.; Ran, C. X.; Wang, M. Q.; Li, L.; Sun, Z. W.; Yao, X. *Phys. Chem. Chem. Phys.* **2016**, *18*, 18219−18226.
(36) Ghaedi, M.; Heidarpour, S.; Kokhdan, S. N.; Sahraie, R.; Daneshfar, A.; Brazesh, B. *Powder Technol.* **2012**, *228*, 18−25.
(37) Xu, X.; Yuan, Y.; Hu, G.; Wang, X.; Qi, P.; Wang, Z.; Wang, Q.; Wang, X.; Fu, Y.; Li, Y.; Yang, H. *Sci. Rep.* **2017**, *7*, 1452.
(38) Sun, J.; Warden, A. R.; Huang, J.; Wang, W.; Ding, X. *Anal. Chem.* **2019**, *91*, 7524−7530.
(39) Sung, Y. J.; Suk, H.-J.; Sung, H. Y.; Li, T.; Poo, H.; Kim, M.-G. *Biosens. Bioelectron.* **2013**, *43*, 432−439.
(40) Srisa-Art, M.; Boehle, K. E.; Geiss, B. J.; Henry, C. S. *Anal. Chem.* **2018**, *90*, 1035−1043.
(41) Adkins, J. A.; Boehle, K.; Friend, C.; Chamberlain, B.; Bisha, B.; Henry, C. S. *Anal. Chem.* **2017**, *89*, 3613−3621.
(42) Chen, J.; Jackson, A. A.; Rotello, V. M.; Nugen, S. R. *Small* **2016**, *12*, 2469−2475.
(43) Wang, S.; Deng, W.; Yang, L.; Tan, Y.; Xie, Q.; Yao, S. *ACS Appl. Mater. Interfaces* **2017**, *9*, 24440−24445.
(44) Kwon, D.; Lee, S.; Ahn, M. M.; Kang, I. S.; Park, K.-H.; Jeon, S. *Anal. Chim. Acta* **2015**, *883*, 61−66.
(45) Alhogail, S.; Suaifan, G. A. R. Y.; Zourob, M. *Biosens. Bioelectron.* **2016**, *86*, 1061−1066.
(46) Safavieh, M.; Ahmed, M. U.; Sokullu, E.; Ng, A.; Braescu, L.; Zourob, M. *Analyst* **2014**, *139*, 482−487.
(47) Bayraç, C.; Eyidoğan, F.; Avni Öktem, H. *Biosens. Bioelectron.* **2017**, *98*, 22−28.
(48) Shim, W. B.; Song, J. E.; Mun, H.; Chung, D. H.; Kim, M. G. *Anal. Bioanal. Chem.* **2014**, *406*, 859−866.
(49) Boulos, S. P.; Davis, T. A.; Yang, J. A.; Lohse, S. E.; Alkilany, A. M.; Holland, L. A.; Murphy, C. J. *Langmuir* **2013**, *29*, 14984−14996.
(50) Dixon, J. M.; Egusa, S. *J. Phys. Chem. C* **2019**, *123*, 10094−10100.
(51) Wang, W. J.; Li, J. J.; Rui, K.; Gai, P. P.; Zhang, J. R.; Zhu, J. J. *Anal. Chem.* **2015**, *87*, 3019−3026.